Original Article

Joint Brain Tumor Segmentation from Multi-magnetic Resonance Sequences through a Deep Convolutional Neural Network

Farzaneh Dehghani[1], Alireza Karimian[1], Hossein Arabi[2]

[1]Department of Biomedical Engineering, Faculty of Engineering, University of Isfahan, Isfahan, Iran, [2]Department of Medical Imaging, Division of Nuclear Medicine and Molecular Imaging, Geneva University Hospital, CH-1211 Geneva 4, Switzerland

Abstract

Background: Brain tumor segmentation is highly contributive in diagnosing and treatment planning. Manual brain tumor delineation is a time-consuming and tedious task and varies depending on the radiologist's skill. Automated brain tumor segmentation is of high importance and does not depend on either inter- or intra-observation. The objective of this study is to automate the delineation of brain tumors from the Fluid-attenuated inversion recovery (FLAIR), T1-weighted (T1W), T2-weighted (T2W), and T1W contrast-enhanced (T1ce) magnetic resonance (MR) sequences through a deep learning approach, with a focus on determining which MR sequence alone or which combination thereof would lead to the highest accuracy therein. **Methods:** The BraTS-2020 challenge dataset, containing 370 subjects with four MR sequences and manually delineated tumor masks, is applied to train a residual neural network. This network is trained and assessed separately for each one of the MR sequences (single-channel input) and any combination thereof (dual- or multi-channel input). **Results:** The quantitative assessment of the single-channel models reveals that the FLAIR sequence would yield higher segmentation accuracy compared to its counterparts with a 0.77 ± 0.10 Dice index. As to considering the dual-channel models, the model with FLAIR and T2W inputs yields a 0.80 ± 0.10 Dice index, exhibiting higher performance. The joint tumor segmentation on the entire four MR sequences yields the highest overall segmentation accuracy with a 0.82 ± 0.09 Dice index. **Conclusion:** The FLAIR MR sequence is considered the best choice for tumor segmentation on a single MR sequence, while the joint segmentation on the entire four MR sequences would yield higher tumor delineation accuracy.

Keywords: *Brain tumor, deep learning, magnetic resonance sequence, segmentation*

Submitted: 21-Apr-2023 **Revised:** 07-Jul-2023 **Accepted:** 31-Jul-2023 **Published:** 08-Apr-2024

Introduction

Brain tumor is defined as the abnormal growth of cells in the brain or the central spinal canal.[1] The most common brain tumors are gliomas, typically categorized into high-grade gliomas (HGG) and low-grade gliomas (LGG).[2] Clinicians obtain the necessary information regarding tumor progression, evolution, and response to the therapy by acquiring data from different medical imaging modalities. Magnetic resonance imaging (MRI) is an effective and sensitive imaging modality for the task of tumor, lesion, tissue, and disease identification/characterization owing to its high soft-tissue contrast compared to other modalities such as computed tomography imaging.[3-8]

The brain tumor segmentation process consists of delineation discrimination of the brain tumor tissues from surrounding normal tissues. Accurate and reliable brain tumor segmentation contributes to disease diagnosis, monitoring, and treatment planning.[9] Although manual brain tumor segmentation is frequently performed by radiologists, it is highly cumbersome and time-consuming. This type of brain segmentation from magnetic resonance (MR) images is prone to intra- and inter-rater variations. Consequently, an accurate and reliable automated brain tumor segmentation method is highly required in clinical settings.[10,11]

Automated tissue/organ delineation/identification from anatomical MR images could be conducted through different techniques, consisting of atlas-based, shape-based averaging, principal component analysis (PCA), and active

How to cite this article: Dehghani F, Karimian A, Arabi H. Joint brain tumor segmentation from multi-magnetic resonance sequences through a deep convolutional neural network. J Med Sign Sens 2024;14:9.

Address for correspondence:
Prof. Alireza Karimian, Department of Biomedical Engineering, Faculty of Engineering, University of Isfahan, Isfahan, Iran.
E-mail: karimian@eng.ui.ac.ir

Access this article online

Website: www.jmssjournal.net

DOI: 10.4103/jmss.jmss_13_23

Quick Response Code:

contour approaches.[12,13] The atlas-based method requires a number of templates/atlases with ground-truth tissue/organ label maps to be aligned/deformed to the target MR images.[14,15] The shape-based averaging method relies on the atlas images and the signed distant map calculation for each label in the atlas dataset to identify the target tissue/organ on the target MR.[12] The PCA-based methods tend to reduce the dimensionality of the input data or variability of the target tissue/organ while retaining the significant or representative variations to identify the target tissue/organ.[16] The active contour method is based on the energy minimization of a deformable spline, which is influenced by the image forces and some predefined constraints to iteratively define the target tissue/organ contour.[17] These approaches have exhibited high degrees of success in deep learning versus conventional methods in this context.[18-20]

In recent years, some researchers, by focusing on brain tumor segmentation issue, have developed innovative deep learning-based approaches with highly improved automatic brain tumor identification and delineation. Researchers[11] proposed a complex convolutional neural network (CNN) architecture for the task of brain tumor segmentation from MR images (BraTS 2013), wherein a cascade of two sequential CNN modules was employed for a robust tumor delineation. Researchers[5] ran a similar study on brain tumor segmentation by applying a CNN model together with intensity normalization and data augmentation to enhance the accuracy of the tumor segmentation. They obtained a Dice index of 0.88, 0.83, and 0.77 for the entire, core, and enhancing tumor regions, respectively.

A model is proposed in Arabi and Zaidi[12] based on the U-Net architecture for brain tumor detection and segmentation on 220 MR images from the BraTS 2015 dataset and reported a Dice index of 0.86. In a similar sense, a U-Net architecture for automated brain tumor segmentation and radiomics-based survival prediction is proposed in Isensee *et al.*,[21] where 0.896, 0.797, and 0.732 Dice scores are obtained for the whole tumor, tumor core, and enhancing tumor regions, respectively, on the BraTS 2015 dataset. For brain tumor segmentation, researchers[22] ran a study wherein an unsupervised approach based on graph coloring is proposed. In this study, the pixels in a brain image are considered nodes of graphs, and the difference between the brightness of a couple of pixels is considered edges. Researchers[23] proposed a combination of fuzzy logic and cellular automata (CA) for brain tumor segmentation from the BraTS 2015 dataset.

Different MR sequences could be applied for imaging brain/tumor in a single acquisition session. The segmentation of tumors could be applied separately or jointly on different MR sequences. The BraTS dataset applied in this study consists of brain MR images in the four T1-weighted (T1W), T1W contrast-enhanced (T1ce), T2-weighted (T2W), and FLAIR sequences.

The objective of this study is to develop a deep learning model for automated segmentation of brain tumor from the different MR sequences. To fulfill this objective, enough deep learning models will be developed to perform brain tumor delineation on each MR sequence (single-channel input) and any combination therein (multi-channel input) to determine the most efficient MR sequences independently for this purpose. Introducing the most effective models (single-, dual-, and multiple-channel inputs) and their corresponding MR sequences for the task of automated brain tumor delineation is the primary focus of this study. This study is organized as follows. In the next section, the methodology applied here for brain tumor segmentation is described in detail. Next, the results of the proposed method, followed by a detailed discussion on its performance for brain tumor segmentation are provided.

Materials and Methods

The automatic brain tumor segmentation from the different MR sequences is assessed for different scenarios including training of deep learning models with single-, dual-, triple-, and quad-channel input/inputs. Different combinations of the MR sequences as the input images to the deep learning models are assessed to identify the most effective models in terms of accuracy in brain tumor segmentation.

Dataset

The publicly available BraTS 2020 dataset containing 370 subjects with HGG and LGG brain tumors, each including T1W, T1ce, T2W, and FLAIR images together with a single manually defined tumor mask, is applied in this study. The entire MR sequences are segmented together into necrotic/nonenhancing tumor, peritumoral edema, and enhancing tumor tissues by experienced radiologists (there is only one tumor mask for each subject/patient or the four MR sequences).[24-26]

Preprocessing

Prior to the training of the deep learning models, the MR sequences are equally cropped to remove the background air and the irrelevant tissues. Among all the segmented images of the patients in the BraTS dataset, the largest tumor size is identified in three x, y, and z directions. Because the input image size fed into the deep learning models should be a multiplication of 8, first, the entire MR images (T1W, T1ce, T2W, and FLAIR sequences) were cropped to a 144 × 128 × 96 mm^3 subvolume which encompassed the whole tumor and the neighboring background tissues. Then, the image intensities of the entire MR images (cropped subvolumes) were normalized within a 0–1 range through division by the maximum values of each MR sequence, separately.

Convolutional Neural Network

The ResNet architecture, implemented in the NiftyNet platform, was adopted to build the different tumor

delineation models.[27] The 310 MRI images in four T1W, T1ce, T2W, and FLAIR sequences are applied as the inputs for training the CNN model. The input image size is 144 × 128 × 96, and the architecture is of HighRes3DNet. The ResNet is a CNN architecture, consisting of 20 layers. In the first seven layers, the low-level features like edges are extracted from the input data. In the next seven layers, a dilated convolutional kernel is applied to encode the medium-level features from the input, and the last six layers apply a dilated convolutional kernel to extract the high-level features. A batch normalization and element-wise rectified linear unit are connected to the convolutional layers in the residual blocks. A residual block is constructed by connecting every two convolutional layers using a residual connection.[28,29]

Each one of the 13 CNN models is trained separately. The inputs of these models consist of the 4 T1W, T1ce, T2W, and FLAIR single-channel sequences, 6 T1W + T1ce, T1W + T2W, T1W + FLAIR, T1ce + T2W, T1ce + FLAIR, and T2W + FLAIR dual-channel sequences, and 3 T1W + T1ce + FLAIR, T1W + T2W + FLAIR, and T1W + T1ce + T2W + FLAIR multi-channel sequences. Here, the Adam and Dice-NS (Dice no-square) are applied as the optimizer and loss function, respectively. The learning rate is 0.01 at 15 batch size. The number of training iterations is 10,000, 12,000, and 20,000 for each of the single-, dual-, and multi-channel models, respectively. To improve the performance of this proposed brain tumor segmentation, the dual-channel and multi-channel CNN is applied to the subvolume, and the results are compared with that of the single-channel. In this experiment, each MRI image is trained and optimized separately, enabling the network to determine the image with the best performance for brain tumor segmentation.

Validation

A total of 13 different ResNet models were trained and 60 subjects (each involving four MR sequences) as an external test dataset were employed for the evaluation of the models. To evaluate the performance of these models, the accuracy of the resulting tumor masks was assessed through standard segmentation metrics. The accuracy of segmentation is determined by applying the sensitivity, precision, Dice similarity coefficient, Jaccard index, and Hausdorff distance parameters, calculated through Eqs. 1-5:[30]

$$Sensitivity(S,M) = \frac{|S \cap M|}{|M|} \quad (1)$$

$$Precision(S,M) = \frac{|S \cap M|}{|S|} \quad (2)$$

$$Dice\ similarity\ coefficient = \frac{2 \times |S \cap M|}{|S| + |M|} \quad (3)$$

$$Jaccard\ index = \frac{|S \cap M|}{|S \cup M|} \quad (4)$$

$$Hausdorff\ Distance(S,M) = \max(h(A,M), h(M,S)) \quad (5)$$

$$, \ h(S,M) = max_{s \in S}\ min_{m \in M} \|s - m\|$$

Where S and M are defined as the automatically and the manually segmented region, respectively. Sensitivity is defined as the ratio of the correctly labeled tumor area to the entire area of the reference tumor. Precision is defined as the proportion of the area/volume that the model correctly identified the tumor to the total area of the tumor delineated by the model. The Dice similarity coefficient and the Jaccard index are applied to compare the degree of similarity or difference between the reference segmented tumor and the tumor segmented through this model. The Hausdorff distance is applied to measure the distance between the reference segmented tumor and the segmented tumor through this deep learning model.

Results

The performance of the single-, dual-, and multi-channel deep learning models is assessed through different standard segmentation metrics. The representative binary masks of the brain tumor segmented by the single-channel and multi-channel models are illustrated in Figure 1.

The details of the sensitivity and precision results for the different deep learning models are tabulated in Table 1, and the results of the Dice similarity coefficient, Jaccard index, and Hausdorff distance are tabulated in Table 2.

The results of this metric on all patients' MRI images are illustrated in Figures 2-4 to facilitate the assessment of the Dice performance in different modalities more accurately.

Discussion

MRI imaging is a time-consuming and cumbersome procedure to which the patients are subject. Identifying MRI sequences with remarkable performance is of great concern for clinical applications. The objective of this study is to find MRI sequences with the best performance for brain tumor segmentation as to avoid unnecessary assessment of imperfect sequences for this purpose. To this end, the performance of the different single- and multi-channel deep learning models was evaluated for the task of automated brain tumor segmentation from the different MR sequences.

The results of sensitivity and precision reveal that this proposed CNN approach is highly reliable for brain tumor segmentation, indicating the acceptable performance of T1ce + FLAIR and T1W + T2W + T1ce + FALIR, respectively [Table 1]. As observed in this table, the T1W, T2W, and T1ce sequences' performance is improved when fused with the FLAIR sequence.

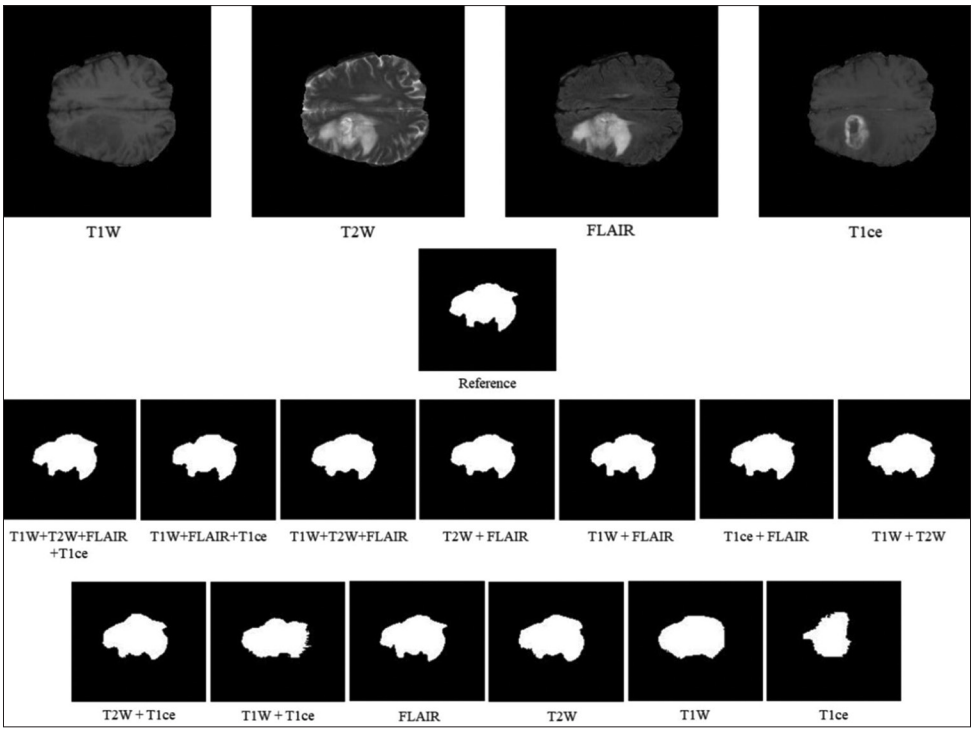

Figure 1: Representative binary mask of the brain tumor segmented by the single-channel and multi-channel models

Table 1: The results of sensitivity and precision for the different single- and multi-channel deep learning models for brain tumor segmentation

Mode	Mean±SD (minimum–maximum)	
	Sensitivity	Precision
FLAIR + T1W + T2W + T1ce	0.80±0.13 (0.48–0.98)	0.87±0.09 (0.48–0.98)
FLAIR + T1W + T2W	0.76±0.17 (0.31–0.98)	0.90±0.08 (0.46–0.98)
FLAIR + T1W + T1ce	0.77±0.15 (0.41–0.97)	0.84±0.10 (0.34–0.98)
T2W + FLAIR	0.82±0.13 (0.44–0.98)	0.80±0.12 (0.27–0.97)
T1W + FLAIR	0.81±0.13 (0.45–0.98)	0.78±0.12 (0.26–0.95)
T1ce + FLAIR	0.85±0.12 (0.57–0.99)	0.73±0.15 (0.22–0.94)
T1W + T2W	0.73±0.18 (0.27–0.98)	0.82±0.13 (0.36–0.97)
T2W + T1ce	0.79±0.14 (0.43–0.97)	0.76±0.14 (0.22–0.94)
T1W + T1ce	0.72±0.13 (0.34–0.92)	0.61±0.15 (0.20–0.83)
FLAIR	0.83±0.12 (0.55–0.99)	0.74±0.14 (0.24–0.92)
T1W	0.79±0.16 (0.19–0.97)	0.69±0.12 (0.29–0.89)
T2W	0.73±0.18 (0.31–0.98)	0.77±0.17 (0.27–0.97)
T1ce	0.68±0.121 (0.09–0.94)	0.60±0.16 (0.07–0.83)

SD – Standard deviation; T1W – T1-weighted; T1ce – T1-weighted contrast-enhanced; T2W – T2-weighted; FLAIR – Fluid-attenuated inversion recovery

To provide more accurate brain tumor segmentation, Dice similarity coefficient, Jaccard index, and Hausdorff distance are calculated. The results obtained from Dice reveal that the performance of all dual/multi-channel CNNs is more reliable than that of the single-channel CNNs, except for T1W + T1ce and FLAIR. The results obtained from Dice and Jaccard indicate that T1W + T2W + T1ce + FLAIR and T1W + T2W + FLAIR CNNs are more reliable than that of the other sequences for brain tumor segmentation. Considering the single- and dual-channel models, the FLAIR and T2W + FLAIR sequences as input images resulted in relatively superior outcomes compared to the other single- and dual-channel models.

The results of the Dice similarity coefficient on all patients' MRI images indicate that multi-channel CNNs are more promising approaches for automated brain tumor segmentation. The main reason for the improved results in joint segmentation is that the different MR sequences provide different representations of the same brain tumor.

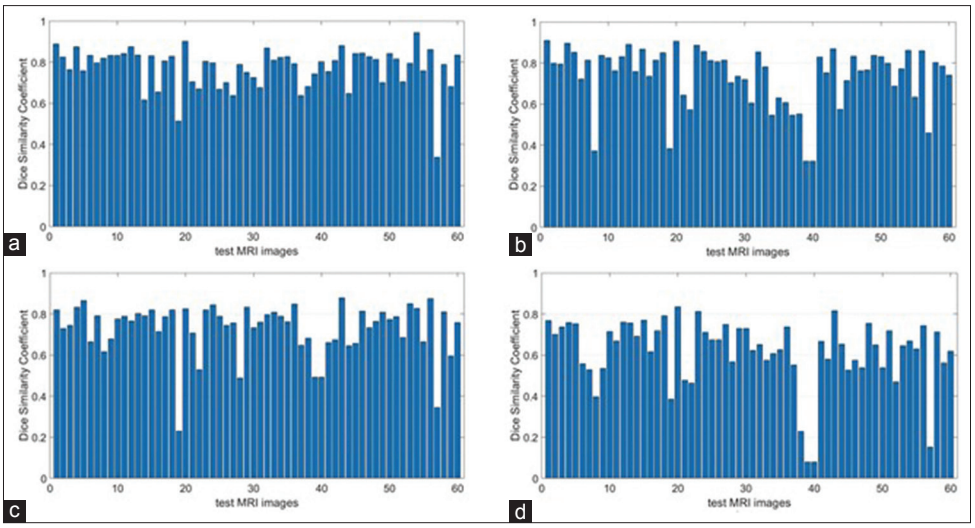

Figure 2: The results of Dice for single-channel magnetic resonance images in the test dataset (a) FLAIR, (b) T2-weighted, (c) T1-weighted (T1W), (d) T1W contrast-enhanced

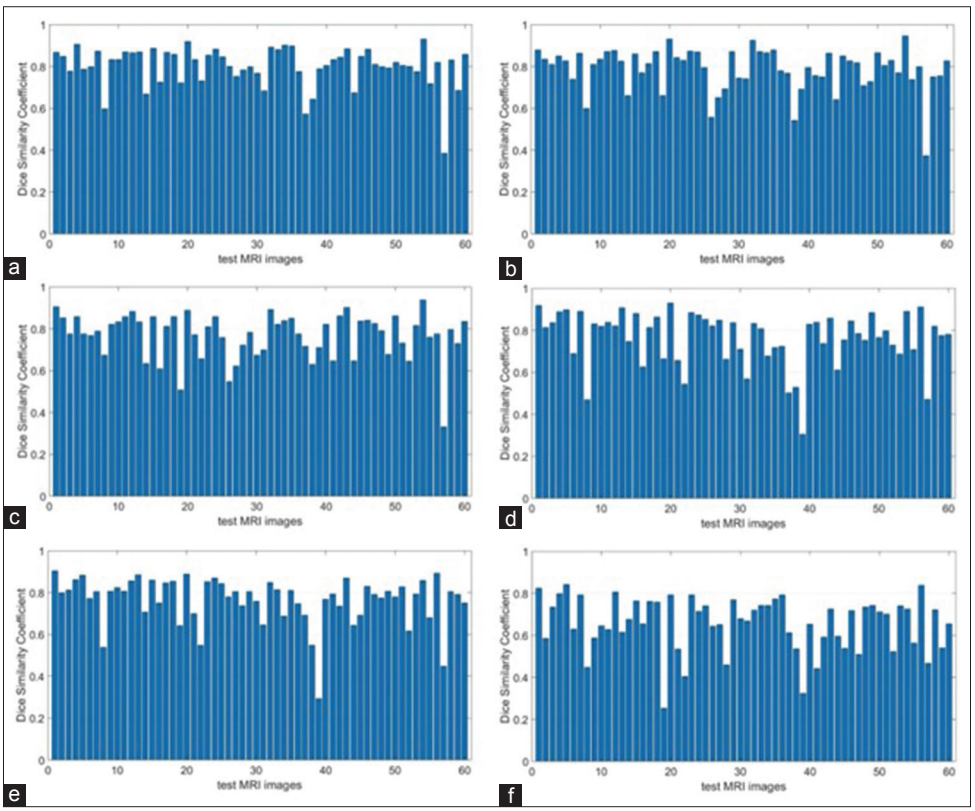

Figure 3: The results of Dice for dual-channel magnetic resonance images in the test dataset (a) T2-weighted (T2W) + FLAIR, (b) T1-weighted (T1W) + FLAIR, (c) T1W contrast-enhanced (T1ce) + FLAIR, (d) T1W + T2W, (e) T2W + T1ce, (f) T1W + T1ce

Thus, the multi-channel models would benefit from the complementary information that exists in the different MR sequences and, as a result, would lead to a more accurate brain tumor delineation. As observed in Figure 2, the Dice indices when using the T1ce sequence as a single input were inferior to those of the dual-channel model with T1ce + FLAIR as input [Figure 3].

As to the results obtained from the single-channel models, it is deduced that the FLAIR sequence bears the most effective information related to the discrimination of the tumor tissue from the background healthy tissues. The T1W, T2W, and T1ce sequences contain less discriminative features for the identification of brain tumors, while each one of these MR sequences provides a unique set of image features

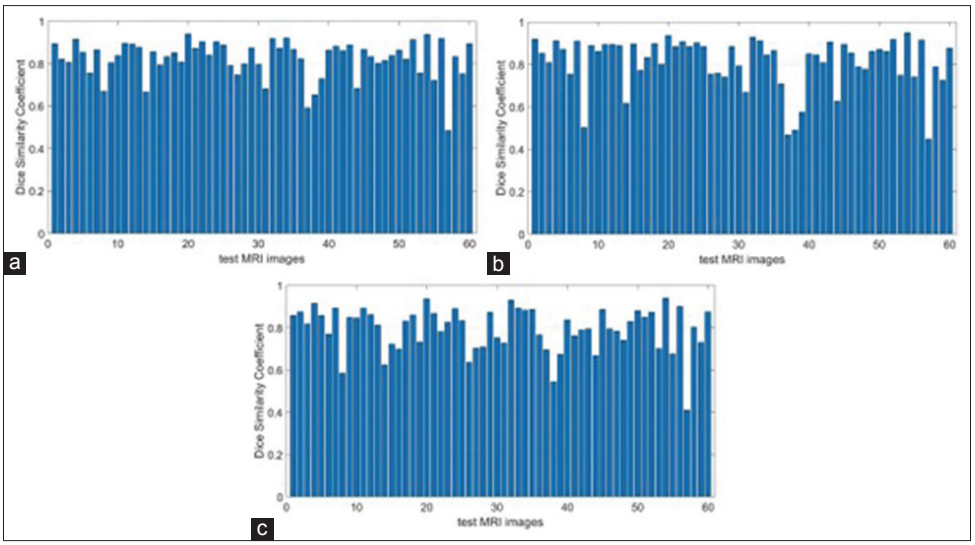

Figure 4: The results of Dice for multi-channel MRI images in the test dataset (a) T1-weighted (T1W) + T2-weighted (T2W) + FLAIR + T1W contrast-enhanced (T1ce), (b) T1W + T2W + FLAIR, (c) T1W + T1ce + FLAIR

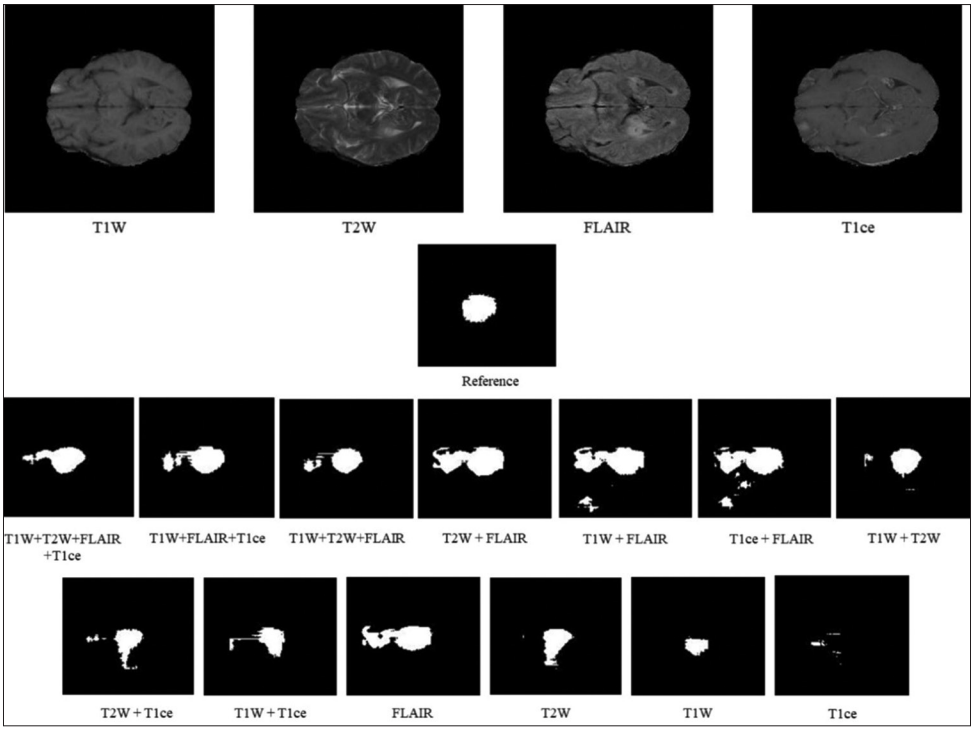

Figure 5: An example of a magnetic resonance image where the deep learning models for brain tumor segmentation failed

to distinguish the tumor from the normal tissues. These image features are not common in the four MR sequences; therefore, the multi-channel model took advantage of all four MR images resulting in the highest tumor segmentation accuracy. Because tumor representation varies in different MR sequences, a combination of these MR sequences would provide a synergy for optimal brain tumor identification.

The Dice score was employed as a metric to compare the performance of the proposed approach with previous attempts at brain tumor segmentation. In Arabi and Zaidi[5,12] and Isensee *et al.*'s studies,[21] where CNN was utilized, the proposed approaches achieved Dice scores of 0.88, 0.86, and 0.89 for whole tumor segmentation, respectively. In this case, the 4-channel model achieved a Dice score of 0.82, which is comparable to the aforementioned studies. Furthermore, despite fusing only two sequences in the T2 + FLAIR model, it yielded a high Dice score of 0.80, indicating the superior performance of this proposed approach on the dual-channel CNN in comparison to the 4-channel CNNs in previous studies. In Mehranian *et al.* and Bagheri *et al.*,[22] a graph coloring approach was employed for brain tumor segmentation, resulting in a Dice score of

Table 2: The results of DICE, Jaccard, and Hausdorff distance for the different single- and multi-channel deep learning models for brain tumor segmentation

Mode	Mean±SD (minimum–maximum)		
	Dice	Jaccard	Hausdorff distance
FLAIR + T1W + T2W + T1ce	0.82±0.09 (0.48–0.94)	0.71±0.12 (0.32–0.89)	3.11±0.51 (1.96–4.87)
FLAIR + T1W + T2W	0.81±0.12 (0.45–0.95)	0.70±0.15 (0.29–0.90)	3.01±0.56 (1.80–4.81)
FLAIR + T1W + T1ce	0.79±0.10 (0.41–0.94)	0.67±0.13 (0.26–0.89)	3.31±0.63 (2.28–5.22)
T2W + FLAIR	0.80±0.10 (0.38–0.93)	0.68±0.12 (0.24–0.87)	3.28±0.53 (2.30–5.01)
T1W + FLAIR	0.79±0.10 (0.37–0.94)	0.66±0.12 (0.23–0.90)	3.50±0.74 (2.24–6.63)
T1ce + FLAIR	0.77±0.11 (0.33–0.94)	0.63±0.13 (0.20–0.88)	3.68±0.67 (2.37–5.90)
T1W + T2W	0.76±0.13 (0.30–0.93)	0.63±0.16 (0.18–0.87)	3.25±0.55 (2.37–5.19)
T2W + T1ce	0.76±0.11 (0.29–0.90)	0.63±0.13 (0.17–0.82)	3.64±0.51 (2.84–5.25)
T1W + T1ce	0.66±0.13 (0.25–0.84)	0.50±0.13 (0.14–0.72)	4.01±0.51 (3.13–5.35)
FLAIR	0.77±0.10 (0.34–0.94)	0.64±0.12 (0.20–0.89)	3.65±0.64 (2.30–5.18)
T1W	0.73±0.13 (0.23–0.88)	0.59±0.14 (0.13–0.78)	3.60±0.50 (2.84–5.18)
T2W	0.73±0.15 (0.32–0.91)	0.60±0.16 (0.19–0.83)	3.49±0.51 (2.52–5.26)
T1ce	0.62±0.17 (0.08–0.84)	0.46±0.15 (0.04–0.78)	3.98±0.56 (2.51–5.48)

SD – Standard deviation; T1W – T1-weighted; T1ce – T1-weighted contrast-enhanced; T2W – T2-weighted; FLAIR – Fluid-attenuated inversion recovery

0.83, which demonstrates that our 4-channel model performs on par with this approach. Although our approach cannot be compared to that of Kalantari *et al.*'s study,[23] where a combination of fuzzy logic and CA achieved a remarkable Dice score of 0.99, it still stands as a highly competent method for brain tumor segmentation, surpassing our own method as well as the previously published methods.

Our method boasts several advantages over other approaches for brain tumor segmentation. For the first time, we conducted a comprehensive comparison of various single-, dual-, and multi-channel models to determine the most effective MR sequences for automated brain tumor segmentation. Unlike other studies that focused solely on introducing a model for tumor delineation, we took the initiative to determine the most effective combinations of the different MR sequences to achieve comparable tumor detection/delineation. This method is adaptable to accommodate tumor locations in different MR images. Another advantage of our model is that it can be applied to 3D images, unlike the method proposed by Kalantari *et al.*,[23] where the fuzzy CA is not time-efficient and highly effective for 3D data. CA models, typically constructed on a two-dimensional grid, often fail to capture the relationships between the third dimensions. However, a drawback of using CNN in our study is that these models require high-performance computing resources, which are not universally available and easily accessible, potentially limiting the applicability of these methods. Moreover, although our model demonstrates high performance in brain tumor segmentation, further exploration of other architectures is warranted to enhance the results.

More assessments conducted through the BraTS dataset revealed that the tumor region is not clear in some MRI images; as a result, the brain tumor segmentation error is inevitable in these MR images [Figure 5]. In this figure, the results obtained from Dice are 0.34, 0.15, 0.45, and 0.29 for T1W, T1ce, T2W, and FLAIR, respectively. For the joint segmentation, the results of Dice are 0.47, 0.45, 0.38, 0.37, and 0.33 for T1W + T2W and T1W + T1ce, T2W + T1ce, T2W + FLAIR, T1W + FLAIR, and T1ce + FLAIR, respectively. For T1W + T2W + FLAIR + T1ce, T1W + T2W + FLAIR, and T1W + T1ce + FLAIR, the results of Dice are 0.48, 0.45, and 0.41, respectively. Although the results are imperfect, dual- and multi-channel sequences outperform the single-channel sequences.

The limited dataset in this study is another challenge. Machine learning has been used for medical imaging applications, such as brain tumor segmentation, to improve the efficiency, reliability, and accuracy of imaging-based diagnosis. However, fundamental challenges such as insufficient annotated data, due to patient privacy and tedious data labeling, hinder the development of ML models for clinical settings. Training CNN network with a large number of data would result in higher performance.

To improve the performance of this proposed approach, we plan to apply other CNN networks on the recently released BraTS 2021 dataset with larger data. In addition, this study was conducted to delineate the entire tumor region. We plan to run a new study to evaluate the performance of our method on tumor core and enhancing tumor regions as well.

For more comprehensive assessments, the performance of multi-MR sequences (3 or 4 inputs) is assessed for brain tumor segmentation. Although the results of multi-MR sequences are enhanced, the extended imaging time is still a real challenge. The objective of this study would be accomplished through the best dual-channel model with T2W + FLAIR sequences as input, where the result of the brain tumor segmentation is increased up to 0.80 in terms of the Dice index.

Conclusion

MRI imaging is highly contributive in disease diagnosis. However, the procedure is time-consuming and cumbersome, especially for patients. Thus, identifying MRI sequences with the high performance could be advantageous for clinical practices. The main aim of this study is to find MRI sequences with remarkable performance for automated brain tumor segmentation. To fulfill this objective, the performance of single- and multi-channel deep learning-based models is evaluated for automated brain tumor segmentation. According to the results, FLAIR sequence would yield higher segmentation accuracy as compared to other sequences (0.77 ± 0.10 Dice index). The model with FLAIR and T2W inputs would result in higher segmentation accuracy for dual-channel models (0.80 ± 0.10 Dice index). As considering multi-channel models, the joint segmentation on the entire four MRI sequences yields the highest segmentation accuracy, with 0.82 ± 0.09 Dice index.

Acknowledgments

The authors would like to thank the University of Isfahan and the Avicenna Center of Excellence (ACE) for their support, subject to contract number 9912011.

Financial support and sponsorship

This work was supported by the University of Isfahan and the Avicenna Center of Excellence (ACE) (grant number: 9912011).

Conflicts of interest

There are no conflicts of interest.

References

1. Raju AR, Suresh P, Rao RR. Bayesian HCS-based multi-SVNN: A classification approach for brain tumor segmentation and classification using Bayesian fuzzy clustering. Biocybern Biomed Eng 2018;38:646-60.
2. Wang G, Li W, Ourselin S, Vercauteren T. Automatic brain tumor segmentation based on cascaded convolutional neural networks with uncertainty estimation. Front Comput Neurosci 2019;13:56.
3. Baur C, Wiestler B, Albarqouni S, Navab N. Deep autoencoding models for unsupervised anomaly segmentation in brain MR images. In: Brainlesion: Glioma, Multiple Sclerosis, Stroke and Traumatic Brain Injuries: 4th International Workshop, BrainLes 2018, Held in Conjunction with MICCAI 2018, Granada, Spain, September 16, 2018, Revised Selected Papers, Part I. Springer Cham: Springer International Publishing; 2019. p. 161-9.
4. Arabi H, Zaidi H. Magnetic resonance imaging-guided attenuation correction in whole-body PET/MRI using a sorted atlas approach. Med Image Anal 2016;31:1-15.
5. Mehranian A, Arabi H, Zaidi H. Vision 20/20: Magnetic resonance imaging-guided attenuation correction in PET/MRI: Challenges, solutions, and opportunities. Med Phys 2016;43:1130-55.
6. Mehranian A, Arabi H, Zaidi H. Quantitative analysis of MRI-guided attenuation correction techniques in time-of-flight brain PET/MRI. Neuroimage 2016;130:123-33.
7. Arabi H, Zaidi H. Truncation compensation and metallic dental implant artefact reduction in PET/MRI attenuation correction using deep learning-based object completion. Phys Med Biol 2020;65:195002.
8. Mostafapour S, Arabi H, Gholamiankhah F, Razavi-Ratki SK, Parach AA. Tc-99m (methylene diphosphonate) SPECT quantitative imaging: Impact of attenuation map generation from SPECT-non-attenuation corrected and MR images on the diagnosis of bone metastasis. Int J Radiat Res 2021;19:299-308.
9. Wadhwa A, Bhardwaj A, Singh Verma V. A review on brain tumor segmentation of MRI images. Magn Reson Imaging 2019;61:247-59.
10. Pereira S, Pinto A, Alves V, Silva CA. Brain tumor segmentation using convolutional neural networks in MRI images. IEEE Trans Med Imaging 2016;35:1240-51.
11. Akkus Z, Galimzianova A, Hoogi A, Rubin DL, Erickson BJ. Deep learning for brain MRI segmentation: State of the art and future directions. J Digit Imaging 2017;30:449-59.
12. Arabi H, Zaidi H. Whole-body bone segmentation from MRI for PET/MRI attenuation correction using shape-based averaging. Med Phys 2016;43:5848.
13. Bahrami A, Karimian A, Fatemizadeh E, Arabi H, Zaidi H. A new deep convolutional neural network design with efficient learning capability: Application to CT image synthesis from MRI. Med Phys 2020;47:5158-71.
14. Arabi H, Zaidi H. Comparison of atlas-based techniques for whole-body bone segmentation. Med Image Anal 2017;36:98-112.
15. Arabi H, Zaidi H. One registration multi-atlas-based pseudo-CT generation for attenuation correction in PET/MRI. Eur J Nucl Med Mol Imaging 2016;43:2021-35.
16. Luo Q, Qin W, Wen T, Gu J, Gaio N, Chen S, *et al.* Segmentation of abdomen MR images using kernel graph cuts with shape priors. Biomed Eng Online 2013;12:124.
17. Fouladivanda M, Kazemi K, Helfroush MS, Shakibafard A. Morphological active contour driven by local and global intensity fitting for spinal cord segmentation from MR images. J Neurosci Methods 2018;308:116-28.
18. Arabi H, Zaidi H. Applications of artificial intelligence and deep learning in molecular imaging and radiotherapy. Eur J Hybrid Imaging 2020;4:17.
19. Arabi H, Bortolin K, Ginovart N, Garibotto V, Zaidi H. Deep learning-guided joint attenuation and scatter correction in multitracer neuroimaging studies. Hum Brain Mapp 2020;41:3667-79.
20. Arabi H, Zaidi H. Deep learning-guided estimation of attenuation correction factors from time-of-flight PET emission data. Med Image Anal 2020;64:101718.
21. Isensee F, Kickingereder P, Wick W, Bendszus M, Maier-Hein KH. Brain tumor segmentation and radiomics survival prediction: Contribution to the brats 2017 challenge. In: Brainlesion: Glioma, Multiple Sclerosis, Stroke and Traumatic Brain Injuries: Third International Workshop, BrainLes 2017, Held in Conjunction with MICCAI 2017, Quebec City, QC, Canada, September 14, 2017, Revised Selected Papers 3. Springer Cham: Springer International Publishing; 2018. p. 287-97.
22. Bagheri R, Monfared JH, Montazeriyoun MR. Brain tumor segmentation using graph coloring approach in magnetic resonance images. J Med Signals Sens 2021;11:285-90.

23. Kalantari R, Moqadam R, Loghmani N, Allahverdy A, Shiran MB, Zare-Sadeghi A. Brain tumor segmentation using hierarchical combination of fuzzy logic and cellular automata. J Med Signals Sens 2022;12:263-8.
24. Menze BH, Jakab A, Bauer S, Kalpathy-Cramer J, Farahani K, Kirby J, *et al.* The multimodal brain tumor image segmentation benchmark (BRATS). IEEE Trans Med Imaging 2015;34:1993-2024.
25. Bakas S, Akbari H, Sotiras A, Bilello M, Rozycki M, Kirby JS, *et al.* Advancing The cancer genome atlas glioma MRI collections with expert segmentation labels and radiomic features. Sci Data 2017;4:170117.
26. Bakas S, Reyes M, Jakab A, Bauer S, Rempfler M, Crimi A, *et al*. Identifying the Best Machine Learning Algorithms for Brain Tumor Segmentation, Progression Assessment, and Overall Survival Prediction in the BRATS Challenge. arXiv Preprint; 2018.
27. Gibson E, Li W, Sudre C, Fidon L, Shakir DI, Wang G, *et al.* NiftyNet: A deep-learning platform for medical imaging. Comput Methods Programs Biomed 2018;158:113-22.
28. Li W, Wang G, Fidon L, Ourselin S, Cardoso MJ, Vercauteren T. On the compactness, efficiency, and representation of 3D convolutional networks: Brain parcellation as a pretext task. In: Information Processing in Medical Imaging: 25th International Conference, IPMI 2017, Boone, NC, USA, June 25-30, 2017, Proceedings 25. Springer Cham: Springer International Publishing; 2017. p. 348-60.
29. Arabi H, Zaidi H. Deep learning-based metal artefact reduction in PET/CT imaging. Eur Radiol 2021;31:6384-96.
30. Taha AA, Hanbury A. Metrics for evaluating 3D medical image segmentation: Analysis, selection, and tool. BMC Med Imaging 2015;15:29.